1975-04

# Experiments in the Initialization of a Global Primitive Equation Model

Haltiner, G.J.; McCollough, J.M.

Journal of Applied Meteorology, Volume 14, pp. 281-288, April 1975.
http://hdl.handle.net/10945/45764

# Experiments in the Initialization of a Global Primitive Equation Model

G. J. Haltiner and J. M. McCollough[1]

*Department of Meteorology, Naval Postgraduate School, Monterey, Calif. 93940*

(Manuscript received 9 August 1974, in revised form 17 December 1974)

ABSTRACT

A global, multi-level, baroclinic primitive equation model is used as a vehicle to test several initialization procedures for suppressing inertial-gravity noise, including static balancing on pressure and on sigma surfaces, iterative dynamic balancing with Temperaton's averaging scheme, and finally the use of a time filter. It is tentatively concluded that static balancing, followed by dynamic balancing equivalent to a 12 h forecast, and the use of a time filter will suppress gravity noise adequately for prediction purposes and may also permit nonsynoptic data to be assimilated about every 4 h without serious trauma.

## 1. Introduction

One of the important problems in numerical weather prediction is the initialization of momentum or primitive equation (P.E.) models. A specific objective in this regard is the reduction of spurious inertial-gravitational "noise" which is a consequence of improperly matched initial mass and velocity fields. A common method of initialization in extratropical regions consists of an objective analysis of the geopotential field by conventional techniques followed by solution of the linear or nonlinear balance equation on pressure surfaces for the streamfunction $\psi$, which, in turn, provides an estimate of the rotational wind component, $\mathbf{V}_\psi = \mathbf{k}\times\nabla\psi$. An alternative approach, used by the National Weather Service, extracts the rotational wind component directly from objectively-analyzed wind observations by calculating the relative vorticity $\zeta$ and then solving the Poisson equation, $\nabla^2\psi=\zeta$, for $\psi$.

In the tropics, where the wind field is usually more reliable than an objectively-analyzed geopotential field, the latter approach is more appropriate from physical considerations. The geopotential field may then be obtained from the previously calculated streamfunction by solution of the balance equation with observed values of $\phi$ utilized to determine boundary points, perhaps interior as well on the edges.

Whatever the method of determining the balanced fields of $\phi$ and $\psi$, the rotational wind component alone is insufficient to eliminate inertial-gravity motion at the onset of a primitive equation forecast. Phillips (1960) utilized a linear, one-layer model permitting both inertial-gravity waves and a low-frequency "meteorological" mode to show that a divergent wind component (quasi-geostrophic in his model) was needed in addition to the rotational wind in order to exclude inertial-gravity wave solutions.

This was confirmed by Temperaton (1973) who demonstrated the existence of inertial-gravity noise with a nonlinear one-layer model which was initialized with the exact rotational wind component (except for truncation and round-off errors). His procedure consisted of integrating the model with the Euler-backward (Matsuno) scheme until the gravitational oscillations were almost completely eliminated. He then continued the integration for an additional 24 h which constituted a "control" run for comparison to results obtained from various methods of initialization for this last 24 h. In one experiment he extracted the rotational wind component from the control winds for the purpose of initializing the model at the beginning of the 24 h control period. All other fields were unchanged except for the omission of the divergent wind component. The results in the form of rms (root mean square) divergence clearly showed the return of spurious inertial-gravity wave oscillations.

Various techniques have been tried to facilitate the geostrophic adjustment process and suppress the gravity noise. A common method consists of integrating forward and backward in time about the initial time (say, $t=0$) while restoring the mass or wind field at $t=0$. Temperaton varied this procedure by first integrating forward $N$ time steps from the initial time, then backward $N$ time steps from the initial time and averaging the two end values of wind velocity, while restoring the geopotential field. He then reversed the procedure by averaging the end values of geopotential and restoring the winds. A value of $N=6$ with 10 cycles of wind averaging, followed by

[1] Lieutenant, U. S. Navy.

10 cycles with geopotential averaging, led to excellent damping of the inertial-gravity modes. However, this is equivalent to a 40 h forecast which is too time-consuming to be practicable in operational forecasting.

A rapid method of effecting geostrophic adjustment is especially important in four-dimensional data assimilation, wherein nonsynoptic reports are incorporated into the analysis-forecast procedure at or very near the time of the report, perhaps every few hours. Such a procedure is necessary if satellite data, which are essentially continuous in time, and other nonsynoptic data are to be utilized in optimum fashion for global analyses. Shortening the time required for geostrophic adjustment is highly important if new data are to be inserted every few hours, or the forecast could be in a continual state of trauma.

Temperaton applied his method of averaging to a nonlinear one-layer model using the shallow water equations. The purpose of this investigation is to apply his technique, as well as several other approaches, to a multilevel baroclinic model, where internal gravity waves probably accomplish much of the adjustment between the mass and motion fields.

## 2. The model

The model used here is global and utilizes a spherical, sigma[2] system of coordinates with the dependent variables staggered both horizontally and vertically. The horizontal velocity components $(u,v)$ and the remaining variables $(w,T,\phi,q,\pi)$ are carried at alternate grid points in the horizontal; while the vertical velocity $w$ is alternated with the other variables at the eleven $\sigma$ levels, $\sigma=0, 0.1, \ldots, 1.0$. The vector equations in sigma coordinates are well known (see, for example, Haltiner, 1971) and will not be repeated here. In general, centered differences are used in conjunction with the staggered grid except for the nonlinear advective terms which are treated by Arakawa's method of averaging which conserves squared quantities and thus avoids nonlinear instability.

Two time-differencing schemes were used, the leapfrog

$$F(t+\Delta t)=F(t-\Delta t)+2\Delta t[\partial F/\partial t]_t,$$

and the Euler-backward, often called the Matsuno scheme

$$\left.\begin{aligned} F^*(t+\Delta t)&=F(t)+\Delta t[\partial F/\partial t]_t \\ F(t+\Delta t)&=F(t)+\Delta t[\partial F^*/\partial t]_{t+\Delta t} \end{aligned}\right\}$$

The latter method has the desirable characteristic of damping high-frequency motions and hence is useful for suppressing inertial-gravity noise. It is also used periodically to restart for the purpose of eliminating the computational mode and solution separation generated by the leapfrog scheme. A time step of 10 min, which insured linear computational stability, was used in all of the experiments. The horizontal spacing between grid points was 5° latitude and longitude. To avoid the shorter time step necessary to maintain linear stability as the east-west lineal distance between grid points decreases toward the poles, the Arakawa technique of Fourier filtering, which decreases the west-east derivatives progressively toward the poles, was used. Specifically, a weighted average is taken of those longitudinal derivatives involved in the propagation of gravity waves, thus permitting a uniform time step without instability.

The model includes diabatic heating in the form of large-scale condensation, cumulus parameterization, solar and terrestrial radiation, sensible heating, convective adjustment and surface friction, orography, and evaporation. The details of these formulations may be found in the description of the Navy Fleet Numerical Weather Central (FNWC) operational Northern Hemisphere model by Kesel and Winninghoff (1972).

[2] $\sigma=p/\pi$, where $\pi$ is surface pressure.

## 3. Data

The data used for the experiments were obtained from FNWC's objective analyses of the Northern Hemisphere which were reflected into the Southern Hemisphere for the purpose of testing the global model. The data consisted of 12 constant pressure analyses, 10 geopotential analyses, four moisture analyses, and sea-level pressure and sea-surface temperature for 1200 GMT 10 May 1972. Terrain heights were relatively unsmoothed.

## 4. Initialization experiments

The initialization experiments included solution of the linear balance equation on pressure surfaces in spherical coordinates for a streamfunction $\psi$, which provided the horizontal wind components

$$u=-\frac{1}{a}\frac{\partial\psi}{\partial\varphi},\quad v=\frac{1}{a\cos\varphi}\frac{\partial\psi}{\partial\lambda}. \tag{1}$$

Sundqvist (1973) suggested that the solution of the balance equation on pressure surfaces followed by interpolation to sigma surfaces creates an imbalance which excited more inertial-gravity oscillations. He therefore proposed direct solution of the balance equation on sigma surfaces and, in limited tests, got less gravity noise. Our investigation therefore included solution of the linear balance equation on sigma surfaces, namely,

$$\nabla\cdot(f\nabla\psi)=\nabla\cdot(\pi\nabla\phi+RT\nabla\pi), \tag{2}$$

which is obtained by taking the divergence of the flux form of the vector momentum equation and assuming zero mass divergence, i.e., $\nabla\cdot\pi\mathbf{V}=0$. The wind components are given by

$$\pi u = -\frac{1}{a}\frac{\partial\psi}{\partial\varphi} \quad \text{and} \quad \pi v = \frac{1}{a\cos\varphi}\frac{\partial\psi}{\partial\lambda}. \tag{3}$$

Since the continuity equation in sigma coordinates may be written in the form

$$\frac{\partial\pi}{\partial t} = -\int_0^1 \nabla\cdot(\pi\mathbf{V})d\sigma, \tag{4}$$

it might be anticipated that gravity waves would be suppressed.

It should be noted that the balance equation is singular at the equator and the pole in spherical coordinates. Solution of the equation by relaxation led to no difficulty near the pole. To avoid the problem on or very near the equator, the streamfunction at 0° was obtained by averaging values at 5°N and 5°S. In addition, the Coriolis parameter was held constant from 10° to the equator in one case and from 20° to the equator in another. The resulting streamfunction field near the equator was of questionable value, but this is probably of little consequence since from practical considerations, the pressure gradients in equatorial regions are likely to be too sensitive to errors and small-scale disturbances to give a reliable large-scale streamfunction consistently. It is therefore more practicable there to compute the vorticity from wind observations, then determine the streamfunction by solution of the Poisson equation, $\nabla^2\psi=\zeta$, and finally calculate the geopotential $\phi$ by solving the balance equation with the known $\psi$.

One of the methods for suppressing inertial-gravity noise has been the use of differencing schemes which have selective damping characteristics. Perhaps the most widely used in this respect is the Euler-backward scheme introduced into meteorological problems by Matsuno (1966). Unfortunately it is a two-step scheme which takes twice as long as the leapfrog scheme; consequently, it has been used sparingly in operational forecasting, mainly to eliminate solution separation by restarting periodically. Temperaton (1973) got no better results in his initialization experiment by starting with the Matsuno scheme than with a simple forward difference. In addition to the Matsuno scheme, the present experiments utilized a time filter (Robert, 1966), i.e.,

$$\bar{F}(t) = F(t) + \alpha[\bar{F}(t-\Delta t) + F(t+\Delta t) - 2F(t)]. \tag{5}$$

The application of this filter together with the leapfrog scheme consists of predicting the value of $F(t+\Delta t)$ as follows:

$$F(t+\Delta t) = \bar{F}(t-\Delta t) + 2\Delta t\left(\frac{\partial F}{\partial t}\right)_t. \tag{6}$$

Now the time filter (5) is applied to determine the averaged value of $F(t)$ and the process is repeated. The filter characteristics have been investigated by Asselin (1972) who showed that high-frequency oscillations are significantly damped while the low-frequency meteorological modes are relatively unaffected. It may be recognized that a value of $\alpha=0.25$ gives the familiar 1-2-1 average, which will eliminate oscillations of periods $2\Delta t$ and halve the amplitude of $4\Delta t$ waves. The amplitude reduction decreases with increasing period; however, the repeated use of the filter does eventually influence periods $\geqslant 12$ h. As a consequence, the computational mode associated with the leapfrog scheme, which essentially has a period of $2\Delta t$, will be eliminated and, in addition, longer period gravitational noise will be suppressed considerably. Various values of $\alpha$, from zero to 0.5, were tested during this investigation, with $\alpha=0.4$ the final choice. The various initialization experiments that were conducted consisted of first obtaining winds from a balance equation, which shall be referred to as *static balancing*, after Mesinger (1972). Then *dynamic balancing* was carried out with the averaging technique of Temperaton, including several different integration schemes and time filters. Finally, the winds obtained by static and dynamic balancing were used to initialize the global model which was integrated forward

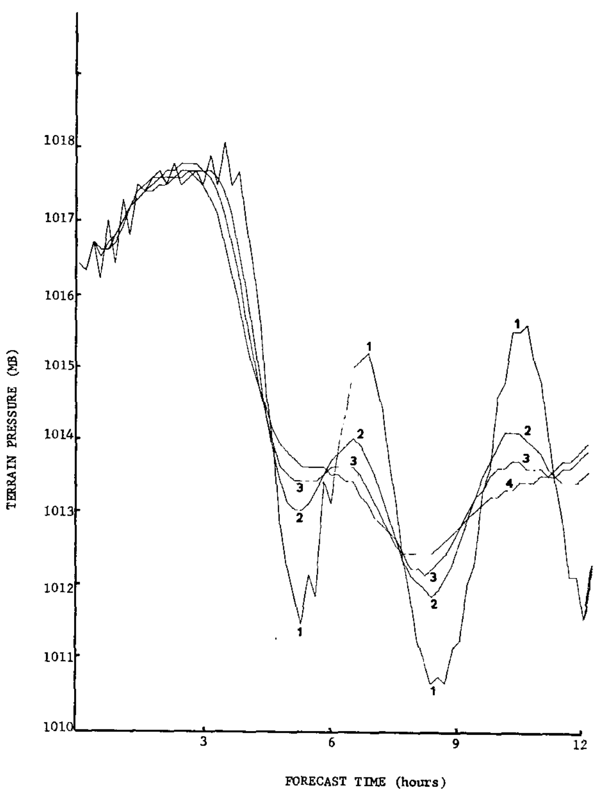


FIG. 1. Terrain pressure versus forecast time at 20°N, 110°E (Experiment 1). Curves 1 through 4, respectively, correspond to the four choices of the time filter parameter, $\alpha=0.0$, 0.3, 0.4, 0.5.

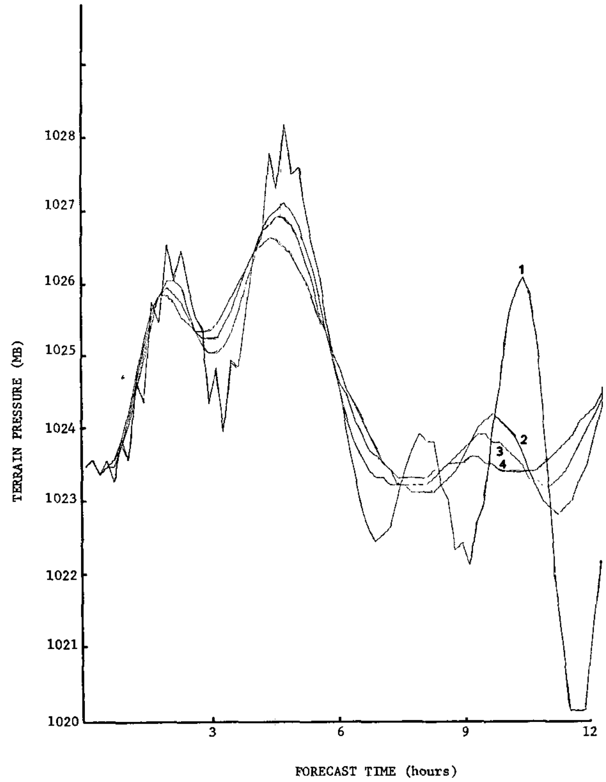


FIG. 2. As in Fig. 1 except at 40°N, 110°E (Experiment 1).

in time out to 72 or more hours. However, only the first 12 h of integration will be discussed here since our primary interest in these experiments was the suppression of inertial-gravity noise.

## 5. Results

The results of five experiments will be described in this section. In each case, initial conditions were established by various combinations of static and dynamic balancing, after which a 12 h forecast was made. In general, the resulting large-scale forecasts were not significantly different; however, the early surface pressure fluctuations, which reflect inertial-gravity noise, differed considerably between some of the experiments. Hence the conventional analyses and forecasts will not be shown; instead, the surface pressure is plotted as a function of time for several randomly chosen grid points.

### *a. Experiment 1*

Four 12 h forecasts were made with balanced initial winds and various choices of the time filter parameter $\alpha$, namely $\alpha=0.0$, 0.3, 0.4, 0.5. A Matsuno time step was taken every 6 h. Figs. 1–3 show the surface pressures as functions of time for the four values of $\alpha$ (in the order given above) at a low-latitude (20°N, 110°E), middle-latitude (40°N, 110°E) and high-latitude point (80°N, 110°E). Note that with $\alpha=0$, there is a pronounced oscillation with a period of about $3\frac{1}{2}$ h at 20°N, several harmonics in evidence at 40°N with peaks separated by about 2–3 h, and a considerably more complicated pattern at 80°N.

It is evident that the time filter is immediately effective in eliminating or reducing the sawtooth variation due to the computational mode. Moreover, the amplitude of the pressure oscillations are sharply reduced after about $4\frac{1}{2}$ h with the maximum reduction for $\alpha=0.5$ (Curve 4), as might be expected. Primary attention should be paid to the 40°N point since the basic FNWC model, from which the global model was adapted, has performed quite well in middle latitudes. On the other hand, there has been little opportunity to verify the model adequately in low latitudes and our treatment of the polar point needs improvement because of a tendency to overdevelop systems there, especially by 72 h. Despite the latter difficulty, it is felt that the experiments are valid indicators of the usefulness of the various initialization procedures.

### *b. Experiment 2*

Experiment 2 was similar to Experiment 1 except that a Matsuno step was taken every hour, every 2 h and every 3 h, with $\alpha=0$. The results were quite

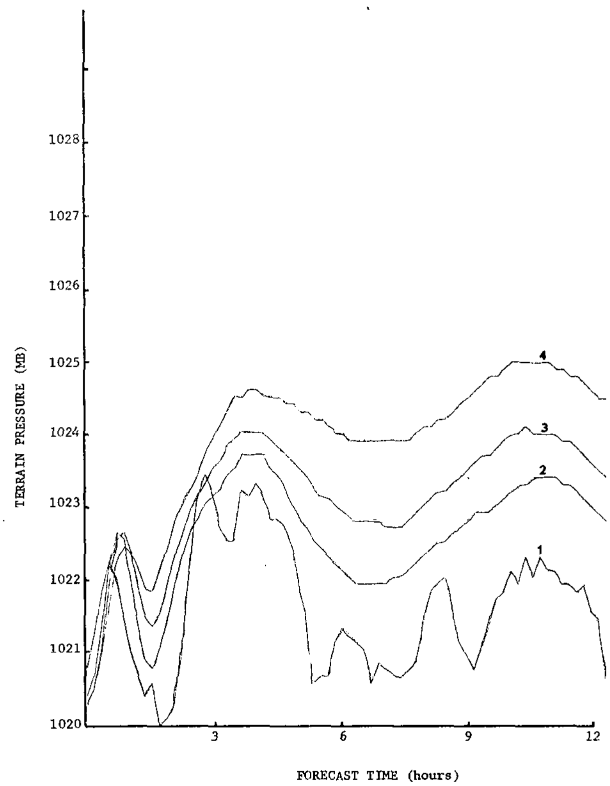


FIG. 3. As in Fig. 1 except at 80°N, 110°E (Experiment 1).

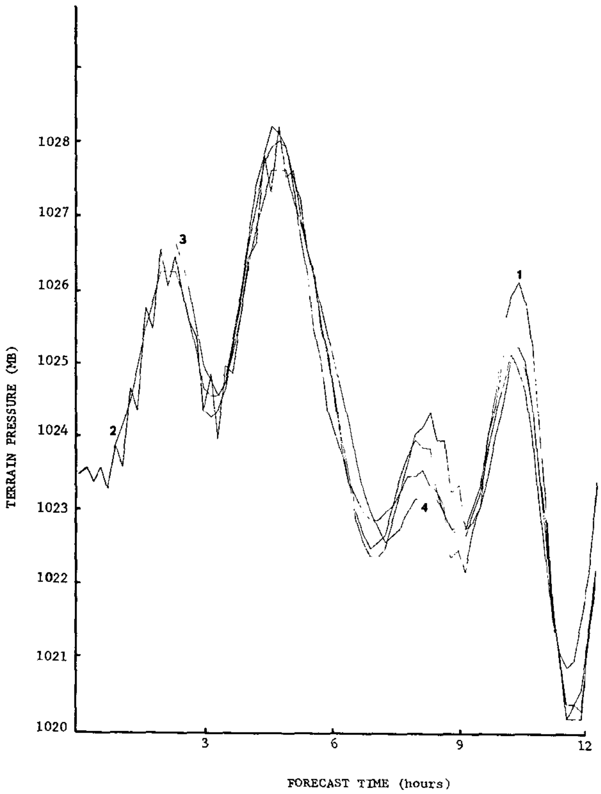


FIG. 4. Terrain pressure versus forecast time at 40°N, 110°E (Experiment 2). Curves 2, 3 and 4 correspond to runs with $\alpha=0$ and a Matsuno time step taken once every 3, 2 and 1 h, respectively. Curve 1 from Fig. 1, with a Matsuno time step every 6 h, is included for comparison.

similar to Experiment 1 with $\alpha=0$. The additional Matsuno steps gave slightly more damping, reducing the amplitude of the oscillations by about 1 mb at most. Further damping could be achieved by more frequent use of the Matsuno scheme, but it is too time-consuming, taking twice as long as the leapfrog scheme. Moreover, it is not as effective as the time filter which takes considerably less computer time to apply. Because of the similarity to the $\alpha=0$ case of Experiment 1, only the curve for 40°N, 110°E is shown for Experiment 2 in Fig. 4. The damping here with increasing use of the Matsuno step from Curves 1 to 4 is typical of the other two latitudes as well.

*c. Experiment 3*

The next experiment combined the time filter ($\alpha=0.4$) with the more frequent use of the Matsuno step to determine if the latter provided enough further damping to justify the additional computer time. Curves 2 in Figs. 5 and 6 show the result at 20°N and 40°N with a Matsuno step every hour, while Curves 3 correspond to a Matsuno step every 6 h, both with $\alpha=0.4$. Curve 1 of Experiment 1 ($\alpha=0$) is also included for comparison. As might have been anticipated from the previous experiment, the increased usage from 1 per 6 hours to 1 per hour does not increase the damping sufficiently to make it worthwhile. This conclusion also holds for the high latitude point as well.

*d. Experiment 4*

The next two 12 h forecasts made were preceded with dynamic balancing by the Temperaton iterative, averaging technique. The curves labeled 1 in Figs. 7 and 8 show the results of 12 h forecasts at 20°N and 40°N with the initial fields determined as follows. First the objectively-analyzed mass field and balanced winds were used to integrate forward 1 h from 1200 GMT and then backward 1 h from 1200 GMT. The resulting winds were averaged while the mass was restored. This dynamic balancing procedure was repeated a total of six times to yield the winds which were then used, along with the original mass field, to make a 12 h forecast. Curves 2 are similar except that the forward and backward integrations were carried out to 3 h before averaging, and the whole cycle was repeated only twice. In both cases the initialization procedure was the equivalent of a 12 h forecast in terms of computer time and the results were quite similar.

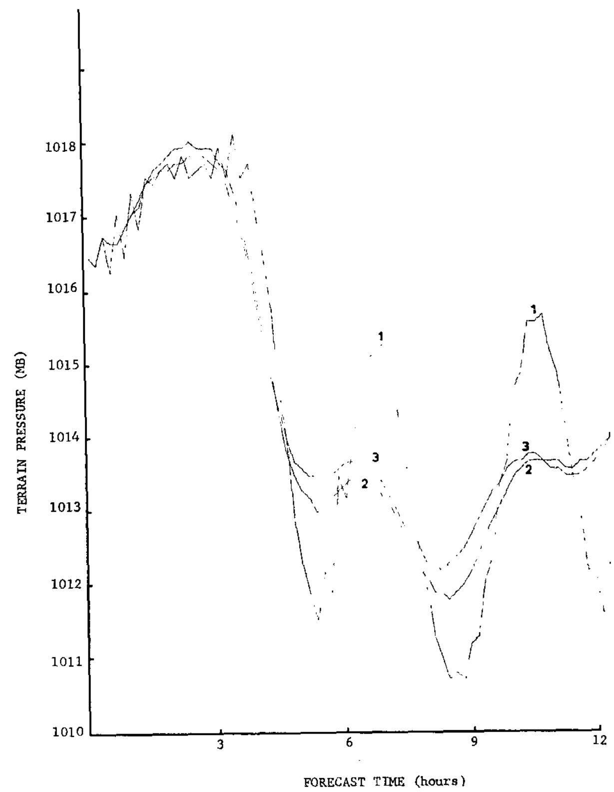


FIG. 5. Terrain pressure versus forecast time at 20°N, 110°E (Experiment 3). Curves 2 and 3 correspond to a Matsuno time step every hour and every 6 h, respectively, both with $\alpha=0.4$. Curve 1 of Fig. 1 with $\alpha=0$ is again included for comparison.

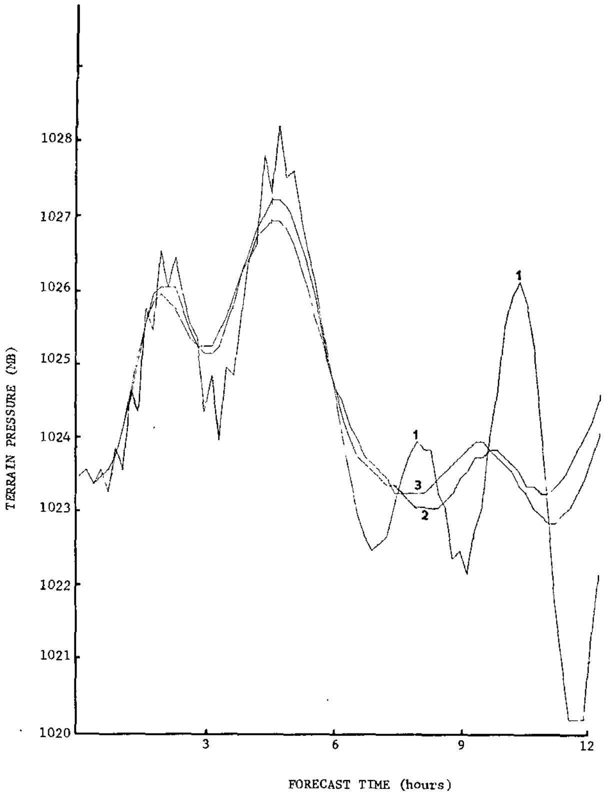


FIG. 6. As in Fig. 5 except at 40°N, 110°E (Experiment 3).

Included for comparison is Curve 3 which represents the case of *no* dynamic balancing, but includes time filtering ($\alpha=0.4$) and one Matsuno time step every 6 h. With dynamic balancing the pressure oscillations are further damped, and after 4–6 h into the forecast, the amplitudes are less than 1 mb. Without dynamic balancing but with a time filter, the oscillations are somewhat greater, about 2 mb after 6 h into the forecast. When a time filter is included, the Matsuno time step for restarting is superfluous and can be omitted.

### *e. Experiment 5*

In this experiment static balancing was carried out by solution of the balance equation on sigma surfaces. For this purpose the mass field variables were first interpolated from pressure surfaces to the sigma surfaces. Then Eq. (2) was solved by a relaxation method to give the streamfunction, from which the winds were computed by means of Eq. (3). Figs. 9 and 10 show the surface pressure as a function of time at 20°N, 110°E and 40°N, 110°E respectively. Curve 1 corresponds to initial pressure-surface balanced winds and Curve 2, the sigma-surface balanced winds. In both cases time filtering was included with $\alpha=0.4$ and a Matsuno time step was introduced every 6 h. Curves 1 differ slightly from the corresponding Curves 3 in Figs. 1 and 2 because orography was not included in these runs. Although the inclusion of orography would provide a more complete evaluation of the sigma balanced winds, it is quite evident that the latter did not reduce the inertial-gravity noise in this experiment when compared to the balancing on pressure surfaces followed by interpolation to sigma levels. Moreover, comparison of Curves 1 with Curves 3 in Figs. 1 and 2 show comparable oscillations in surface pressure at these grid points with and without orography.

## 6. Summary and tentative conclusions

A series of experiments were conducted with several methods of static and dynamic balancing for initializing a global, multi-level, baroclinic primitive equation model for the purpose of reducing the spurious inertial-gravity noise produced by improper matching of the initial mass and wind fields. The results sug-

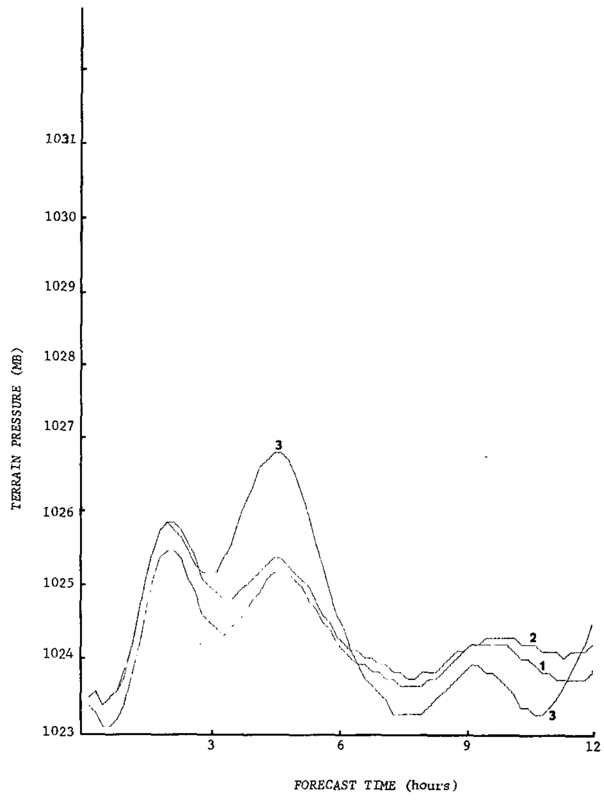


FIG. 7. Terrain pressure versus forecast time at 20°N, 110°E (Experiment 4). Curve 1 results from initial fields obtained by averaging winds from a forward integration of 1 h and a backward integration of 1 h starting with linear balanced winds. The mass field is restored to the initially objectively-analyzed values after each forward and backward step. The foregoing cycle is repeated six times with $\alpha=0.4$. Curve 2 is similar except that the forward and backward integrations are carried out to 3 h and the cycle is repeated only twice. Curve 3 results from no dynamic balancing but with $\alpha=0.4$ and a Matsuno time step every 6 h.

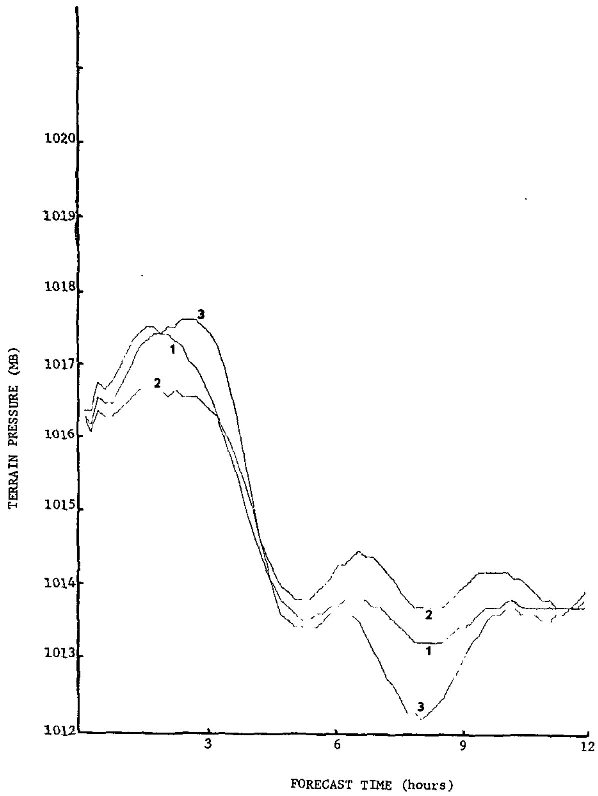


Fig. 8. As in Fig. 7 except at 40°N, 110°E (Experiment 4).

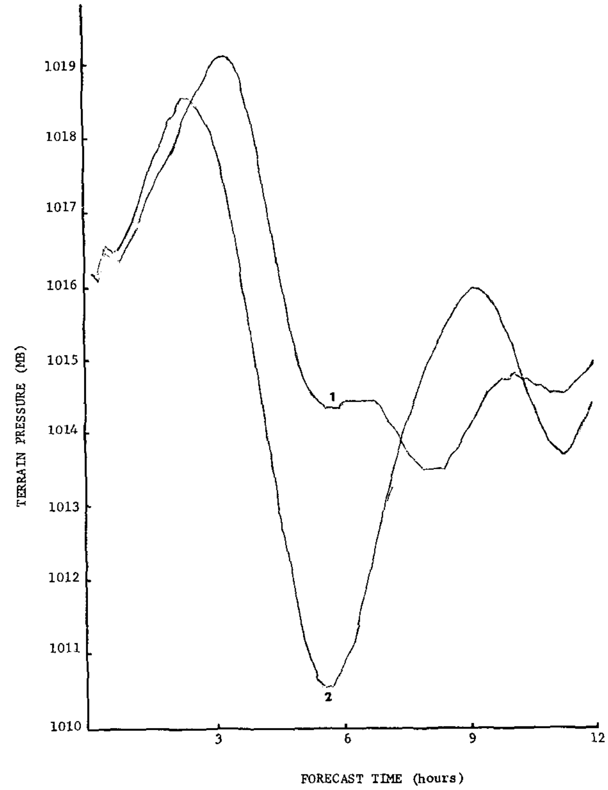


Fig. 9. Terrain pressure versus forecast time at 20°N, 110°E (Experiment 5). Curve 1 corresponds to initial pressure-surface balanced winds and Curve 2 to sigma-surface balanced winds.

gested the following conclusions:

1) The use of sigma-surface linear balanced winds did not give less gravity noise than pressure-surface linear balanced winds in this experiment.

2) A time filter or smoother is quite effective in damping gravitational noise and it essentially eliminates the computational mode, thereby obviating the need for restarting periodically with a forward step such as the Euler backward (Matsuno) scheme (except for the first step).

3) The iterative averaging scheme tested by Temperaton on a one-level "shallow-water" model is also effective in damping gravity noise in a global, multilevel, baroclinic model which admits both external and internal gravity waves.

4) With respect to four-dimensional data assimilation, it appears that static balancing, followed by dynamic balancing coupled with a time filter, is quite effective in suppressing inertial-gravity noise. With this combination, the trauma of initialization can probably be controlled fairly well even if data are inserted every 3 or 4 h. Although divergent wind components were not included along with the balanced rotational wind components prior to dynamic balancing, it is likely that this would enhance the damping process somewhat. For this purpose, a divergent component could be extracted from winds predicted by

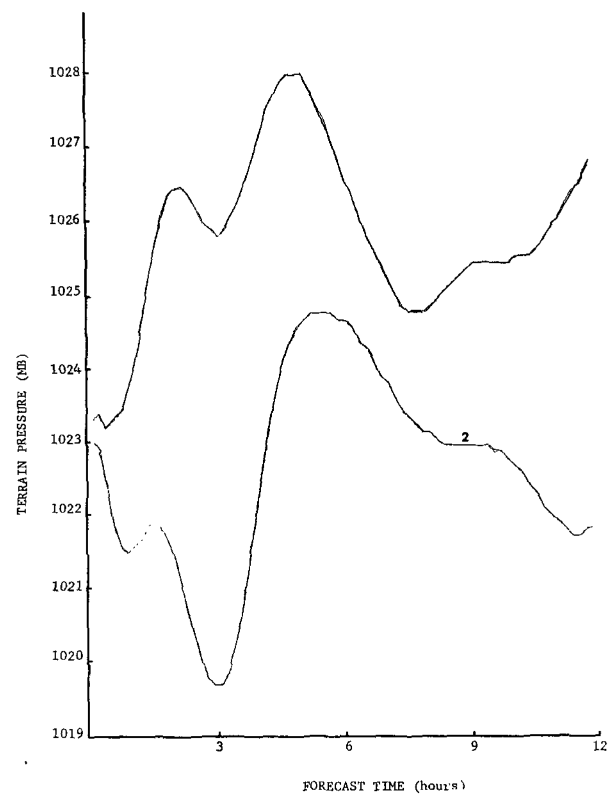


Fig. 10. As in Fig. 9 except at 40°N, 110°E (Experiment 5).

the model from an earlier analysis at virtually no cost in computer time.

Finally, it should be remarked that numerical variational analysis (NVA), which not only provides static balancing but may also include dynamical restraints, can be effective in reducing gravitational noise. It could replace the static balancing and perhaps reduce or even eliminate the need for dynamic balancing. Some experiments with the NVA technique are currently in progress.

*Acknowledgments*. The authors wish to express their gratitude to Prof. R. T. Williams of the Postgraduate School for helpful suggestions during the course of the research and for reading the manuscript. We also wish to thank Lt. W. T. Elias, USN, for assistance in programming the model.

## REFERENCES

Asselin, Richard A., 1972: Frequency filter for time integrations. *Mon. Wea. Rev.*, **100**, 487–490.

Haltiner, G. J., 1971: *Numerical Weather Prediction*, Wiley, 317 pp.

Kesel, P. G., and F. Winninghoff, 1972: The Fleet Numerical Weather Central operational primitive equation model. *Mon. Wea. Rev.*, **100**, 360–373.

Matsuno, T., 1966: Numerical integration of the primitive equations by a simulated backward difference method. *J. Meteor. Soc. Japan*, **44**, 86–88.

Mesinger, F., 1972: Computation of the wind by forced adjustment to the height field. *J. Appl. Meteor.*, **11**, 60–71.

Phillips, N. A., 1960: On the problem of initial data for the primitive equations. *Tellus*, **12**, 121–126.

Robert, Andre J., 1966: The integration of a low-order spectral form of the primitive meteorological equations. *J. Meteor. Soc. Japan*, **44**, 237–245.

Sundqvist, Hilding, 1973: On initialization for models using sigma as vertical coordinate. Rept. DM10, Institute of Meteorology, University of Stockholm.

Temperaton, C., 1973: Some experiments in dynamic initialization for a simple primitive equation model. *Quart. J. Roy. Meteor. Soc.*, **99**, 303–319.